

A Multi-source Information Fusion Approach in Tunnel Collapse Risk Analysis based on Improved Dempster-Shafer Evidence Theory

Bo Wu

Guangxi University

Weixing Qiu (✉ 1910302047@st.gxu.edu.cn)

Guangxi University

Wei Huang

Guangxi University

Guowang Meng

Guangxi University

Jingsong Huang

Guangxi University

ShiXiang Xu

Guangxi University

Research Article

Keywords: Cloud model, Bayesian network, Support vector machine, D-S evidence theory, Tunnel collapse, Safety risk assessment

Posted Date: October 27th, 2021

DOI: <https://doi.org/10.21203/rs.3.rs-1002621/v1>

License: © ⓘ This work is licensed under a Creative Commons Attribution 4.0 International License.

[Read Full License](#)

Version of Record: A version of this preprint was published at Scientific Reports on March 7th, 2022. See the published version at <https://doi.org/10.1038/s41598-022-07171-x>.

1 **A multi-source information fusion approach in tunnel collapse**
2 **risk analysis based on improved Dempster-Shafer evidence**
3 **theory**

4 Bo Wu^{1,2,3}, Weixing Qiu^{1,*}, Wei Huang¹, Guowang Meng¹, Jingsong Huang¹, ShiXiang Xu¹

5 1. College of Civil Engineering and Architecture, Guangxi University, 100 University Road,
6 Nanning, Guangxi 530004, China

7 2. School of Civil and Architectural Engineering, East China University of Technology,
8 Nanchang 330013, Jiangxi, China

9 3. School of Architectural Engineering, Guangzhou City Construction College, Guangzhou
10 510925, Guangdong, China

11 *Corresponding author.

12 E-mail addresses: wubo@gxu.edu.cn (B. Wu), 1910302047@st.gxu.edu.cn (W. Qiu),
13 wei.huang@st.gxu.edu.cn (W. Huang), menggwang@163.com (G. Meng), 164502262@qq.com
14 (J. Huang), 603559081@qq.com (S. Xu)

15
16 **Abstract:** The tunneling collapse is the main engineering hazard in the construction of the drilling-
17 and-blasting method. The accurate assessment of the tunneling collapse risk has become a key issue
18 in tunnel construction. As for assessing the tunneling collapse risk and providing basic risk
19 controlling strategies, this research proposes a novel multi-source information fusion approach that
20 combines Bayesian network (BN), cloud model (CM), support vector machine (SVM), Dempster-
21 Shafer (D-S) evidence theory, and Monte Carlo (MC) simulation technique. Those methods (CM,
22 BN, SVM) are used to analyze multi-source information (i.e. statistical data, physical sensors, and
23 expert judgment provided by humans) respectively and construct basic probability assignments
24 (BPAs) of input factors under different risk states. Then, these BPAs will be merged at the decision
25 level to achieve an overall risk evaluation, using an improved D-S evidence theory. The MC
26 technology is proposed to simulate the uncertainty and randomness of data. The novel approach has

27 been successfully applied in the case of the Jinzhupa tunnel of the Pu-Yan Highway (Fujian, China).
28 The results indicate that the developed new multi-source information fusion method is feasible for
29 (a) Fusing multi-source information effectively from different models with a high-risk assessment
30 accuracy of 98.1%; (b) Performing strong robustness to bias, which can achieve acceptable risk
31 assessment accuracy even under a 20% bias; and (c) Exhibiting a more outstanding risk assessment
32 performance (97.9% accuracy) than the single-information model (78.8% accuracy) under a high
33 bias (20%). Since the proposed reliable risk analysis method can efficiently integrate multi-source
34 information with conflicts, uncertainties, and bias, it provides an in-depth analysis of the tunnel
35 collapse and the most critical risk factors, and then appropriate remedial measures can be taken at
36 an early stage.

37 **Keywords:** Cloud model; Bayesian network; Support vector machine; D-S evidence theory; Tunnel
38 collapse; Safety risk assessment

39

40 **1. Introduction**

41 The highways are extremely important infrastructures for most countries. It ensures
42 communication and development between different regions, especially in the mountains and hilly
43 areas. Most of the surrounding rocks of highway tunnels are mainly hard rock mass, and the
44 geological conditions of the crossing sections are complex and changeable (Sun, 2019). Hard rock
45 tunnels are mostly constructed by drilling and blasting. Due to various risk factors in the complex
46 project environment, safety violations often occur in highway tunnel construction. The collapse is
47 one of the most frequent and harmful geological hazards during the construction of a tunnel. Because
48 the collapse was sudden and instantaneous, it was difficult to predict and the construction workers

49 did not have enough time to escape. Once the tunnel collapse occurs, it may cause serious economic
50 losses, construction delays, and even human casualties. Therefore, it is necessary to research the risk
51 mechanism of tunnel collapse by considering the accident scenario and safety analysis, aiming to
52 provide decision support for assuring the safety of tunnel construction.

53 In recent years, a lot of research work has been carried out in tunnel collapse risk assessment.
54 Zhou (Zhou, 2008) proposed a method for tunnel collapse risk analysis based on the fuzzy Analytic
55 Hierarchy Process. He discussed the collapse mechanism of mountain tunnels and proposed a list
56 of risk factors for tunnel collapse. The Bayesian network is used to conduct a quantitative analysis
57 of safety risks in the Wuhan Yangtze River Metro Tunnel (Zhang, 2014). Wu et al. (Wu et al., 2015)
58 proposed an evaluation method based on a dynamic Bayesian network to provide a real-time
59 dynamic risk assessment for tunnel construction. An optimization method for the preliminary
60 support parameters was proposed based on the genetic algorithm (GA) and combined covariance
61 Gaussian process regression (CCGPR) coupled algorithm presented to provide a complete
62 information-based construction method for tunnel engineering (Liu and Liu, 2019). There are also
63 many studies using artificial intelligence for risk assessment to realize the automation and
64 intelligence of assessment. Pan (Pan and Zhang, 2021) used artificial intelligence to monitor the
65 entire life cycle of real complex projects. The artificial neural networks are used to assess the risk
66 of shield drilling under severe ground conditions such as squeezing grounds (Hasanpour et al., 2020).

67 However, since the above evaluation methods only focus on a single information source, the
68 reliability and accuracy of the security risk assessment cannot be guaranteed. Incomplete
69 consideration of information can lead to inaccurate assessment results, which can not provide
70 accurate recommendations to decision makers (Guo and Zhang, 2021). This would defeat the

71 purpose of the risk assessment. In comparison, the fusion model can greatly improve the accuracy
72 of prediction results due to it has a better understanding of risk factors (Pan et al., 2020). For example,
73 a fusion model is proposed to predict the risk of water inrush disasters (Li et al., 2021). The fusion
74 of sensor data and simulation data improves the accuracy of the structural safety risk assessment
75 (Pan et al., 2020). Nowadays, there has been an increasing interest in the development of modern
76 information technology and Internet technology, which makes the processing and analysis of data
77 from multiple sources particularly important. The data fusion technology may prove to be more
78 helpful to meet the security risk management needs of the tunnel construction than point-based
79 methods (Ding and Zhou, 2013). This research proposes a novel risk assessment approach that
80 integrates Monte-Carlo (MC) simulation technique, normal cloud model (CM), Bayesian networks
81 (BN), probabilistic support vector machine (SVM), and D-S evidence theory. The tunneling collapse
82 risk probability distribution is obtained by analyzing different information sources with different
83 models. Finally, the judgment of each model is fused to give the overall collapse risk result. This
84 model aims to achieve the following goals: (1) Constructing models to estimate the collapse risk
85 according to the expert judgment, monitoring data, and tunneling collapse database; (2) The
86 judgment of the models is fused to get the final collapse risk assessment result; (3) Evaluating the
87 performance of the models to quantify the quality of judgment.

88 **2. Literature review**

89 **2.1 Dempster-Shafer (D-S) evidence theory**

90 Information sources are usually divided into three categories, namely statistical data, physical

91 sensors, and expert judgment provided by humans(Yager, 2016). Among them, statistical data and
92 physical sensors are called hard information. Humans act as soft sensors and execute decision-
93 making processes through a web-based system (Balazs and Velásquez, 2016). Regarding evidence,
94 each source of information constitutes all the evidence on which the decision is based (Leung et al.,
95 2013). In the complex decision-making process, how to compose multiple sources of evidence that
96 may conflict with each other has become a challenging task. So far, over the years, various
97 information fusion researches have been proposed, such as rough set (Qian et al., 2010; Zhang et
98 al., 2021), Dempster-Shafer (D-S) evidence theory (Guo and Zhang, 2021; Leung et al., 2013),
99 maximum entropy approach (Yager, 2016), and others. Among the above-mentioned information
100 fusion methods, D-S evidence theory is an effective and common method in the field of information
101 fusion. Pan et al. (Pan et al., 2020) proposed a risk analysis method based on SVM and D-S evidence
102 theory to fuse different monitoring data, in order to evaluate the structural health status. Zhang et al.
103 (Zhang et al., 2017) developed a novel safety risk assessment method based on D-S evidence theory
104 and the cloud model to perceive the safety risk of buildings adjacent to the tunneling excavation.

105 However, the traditional D-S evidence theory cannot deal with highly conflicting evidence and
106 will lead to unexpected and counter-intuitive results and make the evidence fusion approach
107 insignificant (Zhang et al., 2017). In order to minimize the negative effect of high-conflict evidence,
108 this paper adopted an improved D-S evidence theory by combining the weighted mean rule and the
109 D-S evidence theory to solve the above problem.

110 **2.2 Classification method**

111 For classification problems, support vector machines (SVM) and artificial neural networks

112 (ANN) are the two main supervised learning algorithms in the field of machine learning(Worden
113 and Manson, 2007). Although ANN has provided a powerful tool for the research on tunnel
114 construction (Satpal et al., 2016; Zhou et al., 2016). There are still limitations such as long
115 calculation time, spatial disasters, local minima, overfitting, etc. (Huang, 2009; Pan and Zhang,
116 2021). Due to the small sample of training data for the tunneling collapse case in this paper,
117 classification using neural networks will be prone to overfitting. The support vector machines
118 (SVM), as a method parallel to artificial neural networks (ANN), is a machine learning method
119 established based on the principle of structural risk minimization and the statistical learning theory
120 for a small sample. The SVM has higher accuracy in a small number of training data predictions.
121 Therefore, this article attempts to use SVM to process statistical data for collapse risk assessment.

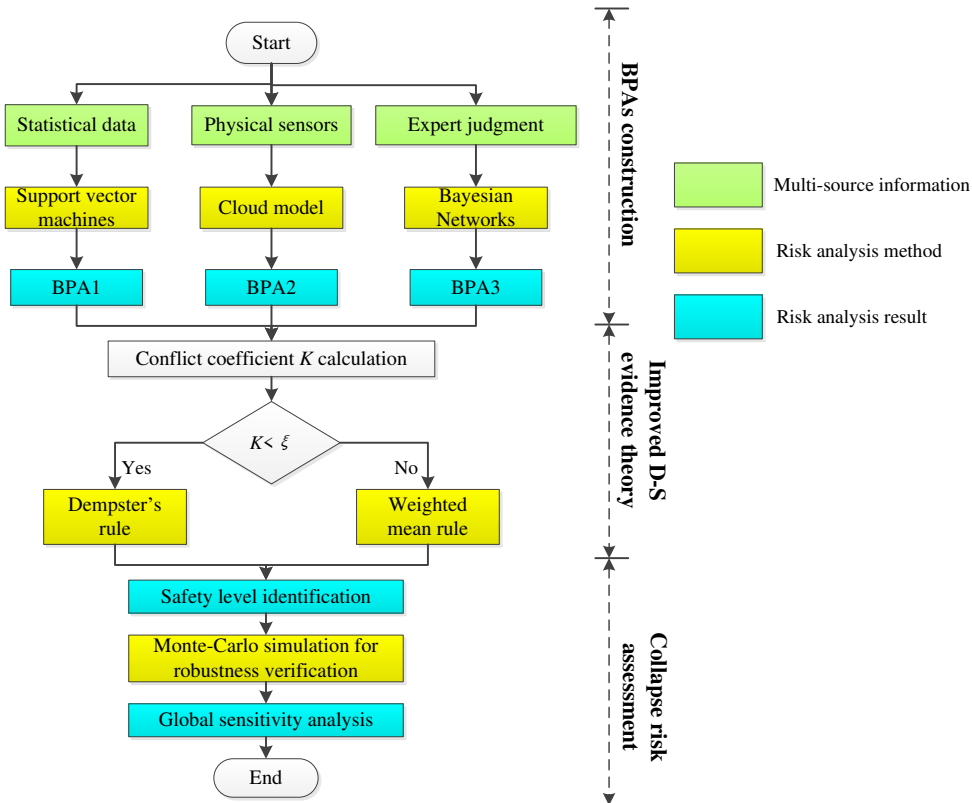
122 **3. Methodology**

123 In order to improve the credibility and robustness of the tunnel collapse risk evaluation, a new
124 hybrid multi-source information fusion method is proposed. Fig. 1 is a flowchart of the tunnel
125 collapse risk analysis method in this paper. In the developed method, all available data from the
126 construction process is collected for risk analysis to improve the accuracy and robustness of the
127 assessment results. In the process of data fusion, an improved D-S evidence theory is utilized to
128 refine and synthesize different classification results generated from probabilistic models. According
129 to the characteristics of different information sources, choose the corresponding probability model.

130 For statistical data, since the statistical data has been classified, SVM with the advantage of
131 small sample classification is used for risk assessment. For physical sensors, quantitative monitoring
132 data needs to be mapped to qualitative collapse risk values. The CM combines fuzzy mathematics

133 and probability theory to map qualitative concepts and quantitative data and is therefore used to
134 process monitoring data during the constructs of BPAs. For expert judgment provided by humans,
135 Bayesian Networks (BN) is used to investigate causal relationships between tunnel collapse and its
136 influential variables based upon the risk/hazard mechanism analysis and expert scores.

137 In collapse risk assessment, the MC simulation can conduct risk analysis by constructing a
138 calculation model containing a series of inherent uncertain variables (Robert and Casella, 2004). It
139 can estimate all possible decision results and evaluate the impact of risks in an uncertain
140 environment (Haronabadi and Haghifam, 2011). The MC simulation is adopted to simulate
141 measurement and human error, proving the robustness of the hybrid approach. A typical hazard
142 concerning the tunnel collapse in the construction of the Fujian Jinzhupa Tunnel in China is
143 presented as a case study. The results demonstrate the feasibility of the proposed approach and its
144 application potential.



145
146 **Fig. 1 Flowchart of the proposed hybrid method for multi-source information fusion decision.**

147 **3.1 BPA construction**

148 3.1.1 Normal cloud model

149 The normal cloud model is a new cognition model of uncertainty, proposed by Li et al. (Li et
150 al., 2009). It can synthetically describe the randomness and fuzziness of elements and implement
151 the uncertain transformation between a qualitative concept and its quantitative value. The normal
152 CM can be determined by numerical characteristics (Ex , En , He). The Expectation “ Ex ” is the
153 expectation of the cloud droplets in the universe of discourse and the typical sample of a qualitative
154 concept. The Entropy “ En ” is the entropy of “ Ex ”, representing the uncertainty measurement of a
155 qualitative concept. Hyper-entropy “ He ” represents the uncertainty degree of Entropy “ En ”.

156 Let X be the universe of discourse and B be a qualitative concept connected with X . If there is

157 a number x , (1) $x \in X$, (2) x is a random instantiation of concept B , (3) x satisfies Eq. (1), the grade
 158 of a certain degree of x belonging to concept B satisfies Eq. (2) (Li et al., 2009):

$$159 \quad \begin{cases} x : N(Ex, En'^2) \\ En' : N(En, He^2) \end{cases} \quad (1)$$

$$160 \quad \mu(x) = e^{-\frac{(x-Ex)^2}{2(En')^2}} \quad (2)$$

161 The tunneling collapse risk assessment is a multi-source information decision-making problem
 162 under uncertain conditions. Various tunnel collapse risk factors B_i are analyzed in the decision-
 163 making process. In order to explore useful information from multiple sources, each risk factor
 164 should be further divided into different risk states B_{ij} ($i=1, 2, \dots, M; j=1, 2, \dots, N$). Each risk state
 165 can correspond to a specific double limit interval, denoted as $[b_{ij}(L), b_{ij}(R)]$. The conversion from
 166 the double limit interval $[b_{ij}(L), b_{ij}(R)]$ to the normal cloud model $(Ex_{ij}, En_{ij}, He_{ij})$ can be achieved
 167 by Eq. (3).

$$168 \quad \begin{cases} Ex_{ij} = \frac{b_{ij}(L) + b_{ij}(R)}{2} \\ En_{ij} = \frac{b_{ij}(R) - b_{ij}(L)}{6}, \quad (i = 1, 2, \dots, M; j = 1, 2, \dots, N) \\ He_{ij} = h \end{cases} \quad (3)$$

169 where, “ Ex_{ij} ” is the expectation; “ En_{ij} ” is the entropy of “ Ex_{ij} ”, “ He_{ij} ” is the Hyper-entropy. The
 170 range of the constant “ h ” is from 0 to “ En_{ij} ” which is adapted to reflects the uncertainty degree of
 171 those factors.

172 In the CM framework, the correlation can measure the relative membership between the
 173 observed value b_{ij} of the factor B_i and the cloud model of a specific risk state B_{ij} . The measurement
 174 of BPAs under different risk states of influential factors can be obtained by Eq. (4) (Zhang et al.,
 175 2017).

$$\begin{cases} m_i(B_j) = \exp\left(-\frac{(x_i - Ex_{ij})^2}{2(En'_{ij})^2}\right), & (i=1,2, \dots, M; j=1,2, \dots, N) \\ m_i(\Phi) = 1 - \sum_{j=1}^N m_i(A_j) \end{cases} \quad (4)$$

177 where, $m_i(B_j)$ is the belief measure; En' represents a random number that satisfies
178 $En' : N(En, He^2)$, and $m_i(\Phi)$ represents the BPAs value in uncertain situations, that is, the focus
179 element cannot be determined under the indicator B_i , so all elements are included.

180 3.1.2 Probabilistic SVM

181 The traditional linear SVM performs linear division by a hyperplane. This hyperplane is found
182 by maximizing the separation margin, which is the distance between the hyperplane and the closest
183 data point. The kernel function is used to map the original data from a low-dimensional space to a
184 feature space with a high-dimensional space, which can obtain better classification accuracy.
185 Besides, the penalty parameter C of the error term also plays a key role in classification accuracy. A
186 high value of C means a strict classifier that does not admit many misclassified points. (Liu et al.,
187 2014). The discrimination function is:

$$f(x) = \text{sign}\left[\left(\sum_{i=1}^m \alpha_i y_i K(x_i, x)\right) + b\right] \quad (5)$$

189 where m is the size of the training data set, α_i represents Lagrange multipliers, $K(x_i, x)$ is a kernel
190 function, and b is a threshold parameter based on the training set.

191 The linear SVM only gives one class prediction output that will be either yes or no. To extract
192 the associated probabilities from SVM outputs, several methods have been proposed. This research
193 chooses Platt's approach (J. Platt, 1999), which uses the Sigmoid function to map the output of the

194 SVM to the interval $[0, 1]$, as given by Eq. (6).

$$195 \quad P(y=1|x) \approx P_{ab}(f(x)) = \frac{1}{1 + e^{(af(x)+b)}} \quad (6)$$

196 where a and b are the parameters computed from the minimization of the negative log-likelihood
 197 function on a set of training examples:

$$198 \quad \min_{z=(A,B)} F(z) = -\sum_{i=1}^l (t_i \log(p_i) + (1-t_i) \log(1-p_i)),$$

$$\begin{cases} t_+ = \frac{N_+ + 1}{N_+ + 2} \\ t_- = \frac{1}{N_- + 2} \end{cases} \quad i = 1, 2, \dots, l \quad (7)$$

199 where t_i is the new label of the classes: +1 becomes t_+ and -1 becomes t_- , N_+ and N_- are the number
 200 of points that belong to class 1 and class 2 respectively.

201 3.1.3 Bayesian network

202 The Bayesian network (BN) is a combination of two different mathematical areas, the
 203 probability theory, and graph theory. It consists of several conditional probability tables (CPT) and
 204 a directed acyclic graph (DAG) (Li et al., 2017). A BN model with n nodes can be represented as
 205 $B\langle G, \Theta \rangle$, where G stands for a DAG with n nodes and Θ is defined as the CPT of the BN model. A
 206 general BN intuitively represents a complex network with n nodes and direct edges. The nodes
 207 $\{X_1, \dots, X_n\}$ in the graph are labeled by related random variables. The directed edges between
 208 nodes represent the relationship between variables. Each node is attached to a CPT that contains the
 209 conditional probability of the parent node.

210 Assuming $parents(X_i)$ is the parent nodes of X_i in DAG, the conditional probability
 211 distribution of X_i is defined as $P(X_i | parents(X_i))$. The calculation of $P(x)$ can be written as Eq.
 212 (8).

213
$$P(x) = P(X_1, L, X_n) = \prod_{X_i \in \{X_1, L, X_n\}} P(X_i | \text{parents}(X_i)) \quad (8)$$

214 **3.2 Improved D-S evidence theory**

215 In this paper, the D-S theory is used to combine multi-source information to obtain the tunnel
 216 collapse risk. Dempster's combinational rule for multiple evidence is calculated with Eq. (9).

217
$$m(B) = \begin{cases} \frac{1}{1-K} \sum_{B_i \perp B_j \perp B_k} m_1(B_i) m_2(B_j) m_l(B_k), & \forall B \subseteq \Theta, B \neq \emptyset \\ 0, & B = \emptyset \\ K = \sum_{B_i \perp B_j \perp B_k} m_1(B_i) m_2(B_j) m_l(B_k) < 1 \end{cases} \quad (9)$$

218 where K is defined to be the normalization factor. l is the number of evidence pieces in the process
 219 of combination, and i, j, k denotes the i th, j th, and k th hypothesis, respectively.

220 When the value of K is close to 1, there will be a high conflict, which means that Dempster's
 221 evidence aggregation rule will be meaningless. To deal with high-conflict evidence, this paper
 222 proposed a hybrid combination rule by combining the weighted mean rule and the Dempster's rule.
 223 This article will use a threshold ζ to indicate high evidence conflicts. When K is greater than ζ , there
 224 is high evidence conflict, and the D-S evidence theory will be replaced by the weighted mean rule,
 225 as shown in Eq. (10). In this research, the value of the threshold ζ is defined to be 0.95 (Zhang et
 226 al., 2017).

227
$$\left\{ \begin{aligned} d &= \sum_{j=1}^{j=l} \sqrt{\sum_{k=1}^{k=L} (m_i(B_k) - m_j(B_k))^2} \\ w_i &= \frac{d_i^{-1}}{\sum_{i=1}^{i=l} d_i^{-1}} \\ \begin{cases} m_i^*(B_k) = w_i g m_i(B_k) \\ m_i(\Theta) = 1 - \sum_{k=1}^L m_i^*(B_k) \end{cases} \end{aligned} \right. \quad (10)$$

228 where l and L are the numbers of evidence and the number of hypotheses, respectively, and k is the
 229 k th hypothesis.

230 3.3 Tunnel collapse risk assessment

231 The collapse risk assessment can provide support for construction decision-making on site.
 232 Once the collapse risk drops to a high-risk level, certain precautions can be taken before the tunnel
 233 collapses. After multiple information sources are fused at the decision-making level, the result of
 234 tunnel collapse risk assessment depends on the maximum value of BPAs, as shown in Eq. (11). The
 235 confidence indicator $m_i(\Theta)$ is designed to measure the credibility of the fusion result.

$$236 \quad \begin{cases} m(B_w) = \max \{m(B_i)\} \\ m(\Theta) < \theta \quad \theta=0.1 \end{cases} \quad (11)$$

237 where B_i denotes collapse risk levels, B_w indicates the probability of different risk levels
 238 $m(B) = \{m(B_1), m(B_2), \dots, m(B_n), m(\Theta)\}$.

239 The sensitivity analysis of the tunneling collapse risk factors is proposed to reveal the
 240 sensitivity of system performance to small changes in risk factors. Up to now, some sensitivity
 241 analysis methods have been proposed (Janssen, 2013). To consider the nonlinearity and interaction
 242 relationship between risk factors, this paper adopts global sensitivity analysis (GSA). Spearman's
 243 rank correlation coefficient (a GSA measure) does not depend on distributions with a similar shape
 244 or being linearly related (Kou et al., 2012). The *GSA* measurement of the i th input factor C_i can be
 245 calculated by Eq. (12).

$$246 \quad GSA(C_i) = \frac{\sum_{p=1}^P (R(x_i^p) - \bar{R}(x_i^p))(R(t^p) - \bar{R}(t^p))}{\sqrt{\sum_{p=1}^P (R(x_i^p) - \bar{R}(x_i^p))^2} \sqrt{\sum_{p=1}^P (R(t^p) - \bar{R}(t^p))^2}} \quad (12)$$

247 where P is the number of the repeated interactions; $R(x_i^p)(R(t^p))$ is the rank of $x_i^p(t^p)$ among

248 the simulated input data; $\bar{R}(x_i^p)(\bar{R}(t^p))$ is the mean value of $R(x_i^p)(R(t^p))$.

249 **4. A case study**

250 The Jinzhupa Tunnel is a twin-tube highway tunnel. The right and left tunnels are 782m and
251 771m long, respectively. This paper takes the left line (ZK242+548~ZK243+319) as the object of
252 study. The fault structure along the left line of the tunnel is shown in Fig. 2. There are 316m of V-
253 level surrounding rock section and 455m of IV-level surrounding rock section. The rock mass is
254 mainly composed of the residual silty clay, granite fully weathered layer, and broken strong
255 weathered layer. Furthermore, there is a fracture fragmentation zone at section ZK243+139~160.
256 Affected by this, the rock mass is relatively broken, showing a huge mosaic structure or broken
257 mosaic structure. The rock mass is broken and has varying degrees of weathering. During the
258 construction process, it is easy to cause tunnel collapse and water burst. Therefore, it is urgent to
259 conduct a collapse risk assessment of the tunnel to reduce the losses caused by the collapse. In the
260 proposed fusion method, the following four steps are adopted:

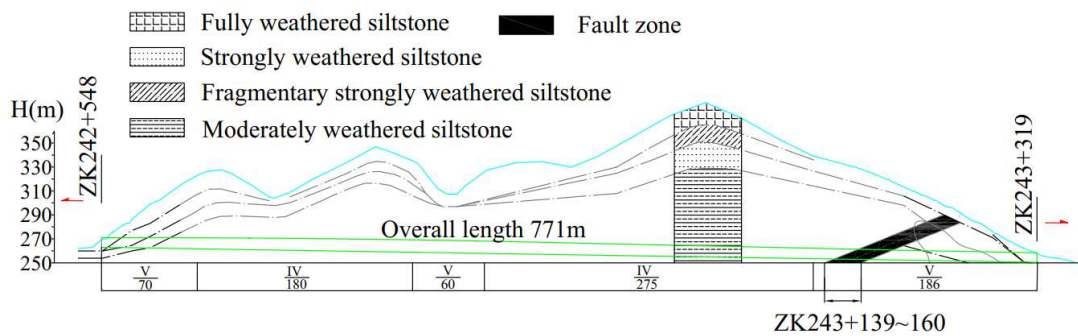
261 Step (1) Collapse risk assessment based on statistical data: The risk mechanism of tunneling
262 collapse is analyzed to reveal the potential risk factors. Then the collected tunneling collapse data
263 set are used to train SVM models.

264 Step (2) Collapse risk assessment based on expert judgment: According to the construction
265 personnel's description of the site situation, the Bayesian network is used to assess the collapse risk.

266 Step (3) Collapse risk assessment based on monitoring data indicator: Using the arch
267 displacement and horizontal convergence displacement monitoring data of the tunnel as the
268 information source, the cloud model is applied for collapse risk assessment.

269 Step (4) Multi-source information fusion: The results of the above three assessment models are
270 used as information sources and fused using the improved D-S theory to obtain the overall tunneling
271 collapse risk value.

272 Step (5) Robustness of risk assessment results: Different percentages of deviation (5%, 10%,
273 15%, and 20%) were added to the collected data. The robustness of the proposed hybrid method is
274 further validated in the presence of unavoidable data biases.



275
276

Fig. 2 Fault structures along the Jinzhupa Tunnel

277 5. Result and analysis

278 5.1 Collapse risk assessment based statistical data

279 (1) Risk/hazard identification in the tunnel collapse

280 In actual engineering, the tunneling collapse may be affected by many factors, which interact
281 with each other. Many scholars(Qiao et al., 2020; Wang et al., 2016, 2020; Zhang et al., 2020) have
282 studied the risk factors of collapse and established a similar index system. Referring to previous
283 researches, a total of 15 risk factors are selected, as shown in Table 1. The risk factors are analyzed
284 in detail as shown in (Zhou, 2008; Zhang et al., 2020). At the same time, the safety status of each
285 tunnel collapse risk factor is divided into four levels, as shown in Table 1.

286

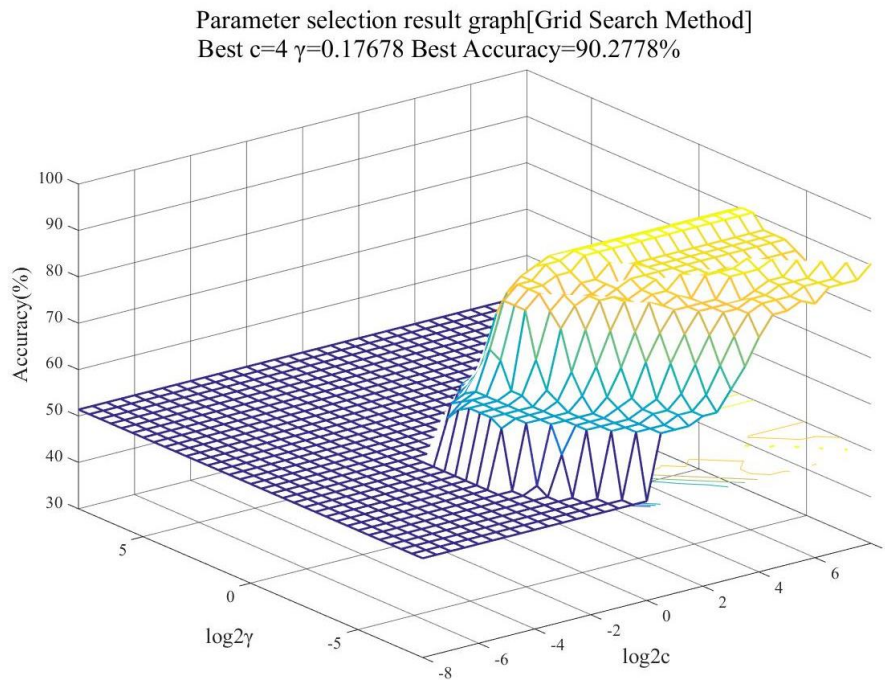
Table 1 Classified states of tunnel collapse risk factors.

Factors	I	II	III	IV
Tunnel collapse (T)	Safe	Deformation	Small-scale collapse	Large-scale collapse
Geometric factor (B_1)	No risk	Low risk	Medium risk	High risk
Geological factors (B_2)	No risk	Low risk	Medium risk	High risk
Construction technology (B_3)	No risk	Low risk	Medium risk	High risk
Construction management factors (B_4)	No risk	Low risk	Medium risk	High risk
Excavation span (m) (X_1)	<7	7-10	10-14	>15
Depth-to-height ratio (H_0/H) (X_2)	>20	15~20	10~15	<10
Rock mass grade (X_3)	I(81~100)	II(61~80)	III(41~60)	IV, V (<40)
Groundwater level ($(H_0+H)/H_w$) (X_4)	<5	5~20	20~35	>35
Unfavorable geology (X_5)	Non-Catastrophability (76~100)	Weak Catastrophability (51~75)	Medium Catastrophability (26~50)	Strong Catastrophability (0~25)
Bias angle ($^\circ$) (X_6)	<10	10~25	25~40	>40
Primary support stiffness (X_7)	Reasonable	Almost reasonable	Unreasonable	Extremely unreasonable
Ground reinforcement measures (X_8)	Accurate	Almost accurate	Inaccurate	Extremely inaccurate
Excavation method (X_9)	CRD	CD	Bench	Full face
Waterproofing and drainage measures (X_{10})	Reasonable	Almost reasonable	Unreasonable	Extremely unreasonable
Timeliness of primary support(min) (X_{11})	<30	30~60	60~120	>120
Monitoring (X_{12})	Reasonable	Almost reasonable	Unreasonable	Extremely unreasonable
Construction quality (X_{13})	Good (76~100)	Fair (51~75)	Poor (26~50)	Very poor (0~25)
Accuracy of geological investigation (%) (X_{14})	>90	75~90	60~75	<60
Rationality of procedure linkage(X_{15})	Reasonable	Almost reasonable	Unreasonable	Extremely unreasonable

288 (2) Choice of kernel function and parameters

289 In order to construct the SVM model, a dataset of 70 tunnel collapses was collected from the
290 study (Zhou, 2008) and classified according to Table 1. The dataset is used as training data, and the
291 optimal hyperparameters (C , γ) of the SVM model are found using the grid search method. Due to

292 the limited input data, the 5-fold cross-validation is conducted to determine the best value of the
 293 penalty parameter C and the gamma γ . Pairs of (C, γ) with different values are tested in the SVM
 294 model, and their corresponding results about the classification accuracy as shown in Fig. 3. The
 295 search range for the optimal hyperparameters (C, γ) is $[2^{-8}, 2^8]$. When the parameter $C=4, \gamma=0.17678$,
 296 the accuracy of classification is the highest.



297
 298 **Fig. 3 Support Vector Machines evaluation accuracy based on pairs of (C, γ) .**

299 (3) Calculation of the collapse risk probability

300 According to Eq. (6), the probability of different collapse risk levels is calculated. Since the
 301 fracture zone is prone to collapse during excavation, this paper assesses the collapse risk of the
 302 fracture zone. In tunnel sections (ZK243+130~330), every 10 meters of the tunnel section is selected
 303 as a testing sample, and 20 samples are taken. The SVM model is utilized to evaluate the collapse
 304 risk value of the testing sample, the classification results as shown in Table 2. The risk level of
 305 tunnel collapse with the highest probability in the bold font in Table 2 represents the classification
 306 result. Despite the high accuracy of the probabilistic SVM evaluation results, it is worth noting that

307 the second-highest probability is very close to the highest value in some of the prediction results.
 308 For example, a tunnel section No.9, the probability of tunnel collapse for class I (0.45) and class II
 309 (0.50) is very close, which means that the results are very uncertain.

310

Table 2 Results of probabilistic Support Vector Machines.

Tunnel section	$m(I)$	$m(II)$	$m(III)$	$m(IV)$	Predicted risk	Ture risk
No.1	0.14	0.60	0.18	0.08	II	II
No.2	0.02	0.02	0.94	0.02	III	III
No.3	0.04	0.91	0.03	0.01	II	II
No.4	0.64	0.30	0.06	0.00	I	II
No.5	0.04	0.91	0.03	0.02	II	II
No.6	0.03	0.91	0.04	0.02	II	II
No.7	0.07	0.87	0.04	0.02	II	II
No.8	0.91	0.03	0.03	0.03	I	I
No.9	0.45	0.50	0.02	0.03	II	I
No.10	0.83	0.09	0.04	0.04	I	I
No.11	0.03	0.89	0.05	0.03	II	II
No.12	0.01	0.93	0.01	0.05	II	III
No.13	0.87	0.08	0.03	0.02	I	I
No.14	0.92	0.04	0.02	0.02	I	I
No.15	0.05	0.91	0.02	0.01	II	II
No.16	0.87	0.08	0.02	0.02	I	I
No.17	0.05	0.90	0.03	0.02	II	II
No.18	0.86	0.08	0.03	0.03	I	I
No.19	0.91	0.03	0.03	0.03	I	I
No.20	0.03	0.91	0.04	0.02	II	II

311 5.2 Collapse risk assessment based on expert judgment

312 (1) Establishment of the DAG and CPT

313 The DAG is mainly constructed by directed edges and node variables that represent the
 314 probability causality between node variables. In combination with the risk factors in Table 1, the
 315 DAG can be established, as shown in Fig. 4. To reduce the uncertainty of expert judgment, an expert
 316 survey based on confidence index is used to construct the conditional probability tables (CPT), the
 317 detail as seen in (Zhang et al., 2020).

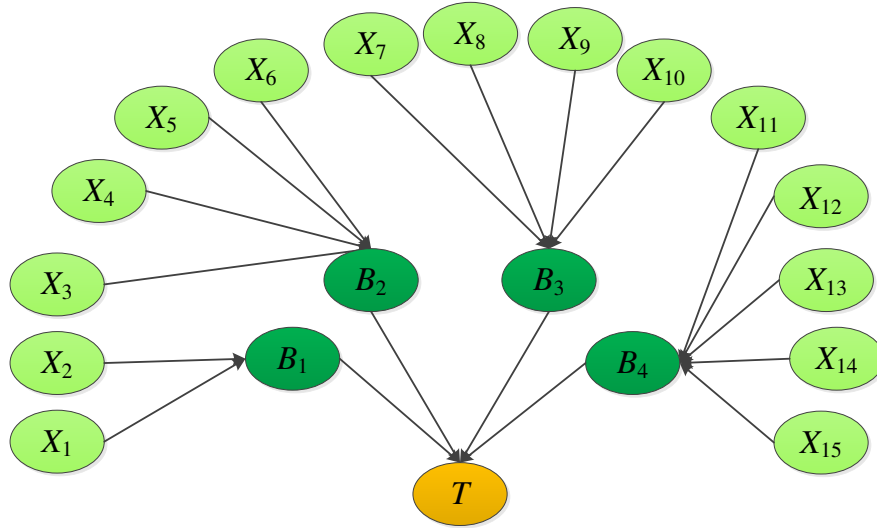


Fig. 4 DAG of Bayesian network.

(2) Calculation of the tunneling collapse risk

Similarly, taking the above 20 sections as examples, Eq. (8) is used to obtain the probability of their collapse risk value, the result as shown in Table 3. Compared with the prediction results of the probability SVM, the accuracy of the model is lower. The second-highest probability in some prediction results is also very close to the highest value. For example, a tunnel section No.1, the probability of tunnel collapse for class II (0.48) and class III (0.52) is very close, which means that the results are very uncertain.

Table 3 Results of Bayesian network at ten monitoring sections.

Tunnel section	$m(I)$	$m(II)$	$m(III)$	$m(IV)$	Predicted level	Ture level
No.1	0.00	0.48	0.52	0.00	III	II
No.2	0.00	0.00	0.93	0.07	III	III
No.3	0.00	0.70	0.30	0.00	II	II
No.4	0.00	0.96	0.04	0.00	II	II
No.5	0.00	0.96	0.04	0.00	II	II
No.6	0.78	0.22	0.00	0.00	I	II
No.7	0.00	0.97	0.03	0.00	II	II
No.8	0.84	0.16	0.00	0.00	I	I
No.9	0.19	0.81	0.00	0.00	II	I
No.10	0.87	0.13	0.00	0.00	I	I
No.11	0.00	0.99	0.01	0.00	II	II
No.12	0.00	0.01	0.83	0.17	III	III
No.13	0.96	0.03	0.01	0.00	I	I
No.14	0.65	0.35	0.00	0.00	I	I

No.15	0.07	0.93	0.00	0.00	II	II
No.16	0.33	0.67	0.00	0.00	II	I
No.17	0.01	0.98	0.00	0.00	II	II
No.18	0.66	0.33	0.01	0.00	I	I
No.19	0.18	0.82	0.00	0.00	II	I
No.20	0.00	0.93	0.07	0.00	II	II

328 **5.3 Collapse risk assessment based on monitoring data indicator**

329 (1) Monitoring data indicator system

330 The monitoring measurement data includes the displacement of the vault, the surface
331 settlement of the shallow buried section, and the change of the surrounding rock convergence. These
332 data can reflect the stability of the tunnel support after the initial lining, thereby assessing the risk
333 of collapse. Combined with this project, the vault displacement and the convergence displacement
334 are used to analyze the collapse risk. According to the Chinese standards “Technical code for
335 monitoring measurement of highway tunnel (DB 35/T 1067-2010)” and “Technical specification for
336 construction of highway tunnel (JTG/T 3660-2020)”, the daily deformation rate and cumulative
337 deformation of the two-monitoring data are divided into four levels, as shown in Table 4.

338 **Table 4 Classified states of monitoring measurement data.**

Tunnel collapse level	I (Safe)	II (Deformation)	III (Small-scale collapse)	IV (Large-scale collapse)
Daily deformation rate (mm/d)	$0 \leq x < 2$	$2 \leq x < 5$	$5 \leq x < 10$	$10 \leq x \leq 20$
Cumulative deformation (mm)	$0 \leq y < 50$	$50 \leq y < 100$	$100 \leq y < 200$	$200 \leq y \leq 300$

339 where, the cumulative deformation (y) should be multiplied by the coefficient (ζ) according to the
340 distance between the measuring point and the excavation surface (D), the detail as shown in Table
341 5.

342

343

Table 5 The coefficient (ζ) of the cumulative deformation (y).

The distance between the measuring point and the excavation surface (D)	$1B$	$2B$	$3B$	$4B\sim 4B$
ζ	0.5	0.75	0.85	1

344

where B is the face span of the excavation section.

345

(2) Monitoring data collection

346

The tunnel is excavated by the bench method, and the monitoring points and measuring points

347

are arranged as shown in Fig. 5. Among them, point A, B, and C are the monitoring points for the

348

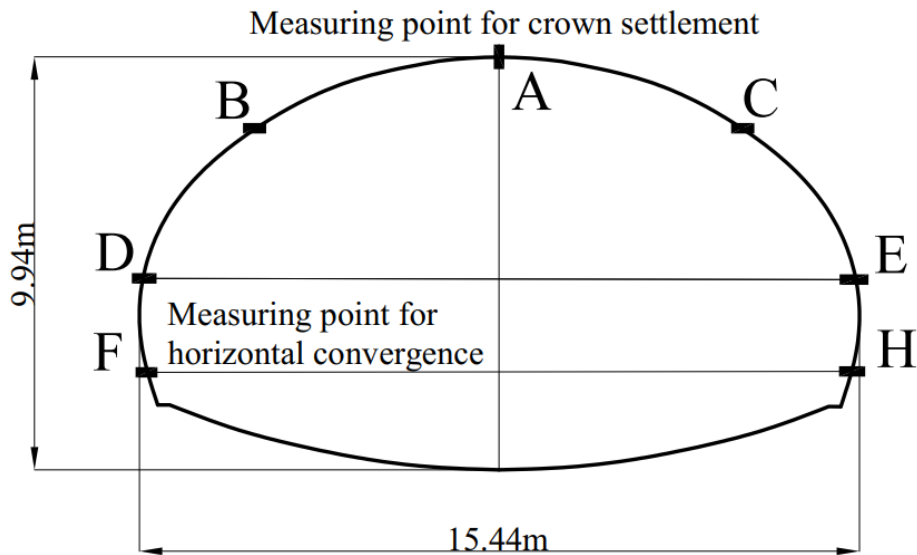
settlement of the vault, DE and FH are the surrounding rock convergence line. The surrounding rock

349

displacement is monitored once in the morning and once in the evening, and the average value is

350

taken as the monitoring value of the day.



351

352

Fig. 5 Schematic diagram of monitoring point layout.

353

(3) Calculation of the tunneling collapse risk

354

According to Eq. (3), the cloud model parameter values (Ex, En, He) of the two monitoring

355

indicators are constructed, as shown in Table 6. Finally, the tunnel collapse risk BPAs is constructed

356

by Eq. (4).

357

The cloud model is used to obtain the BPAs of the cumulative settlement and daily settlement

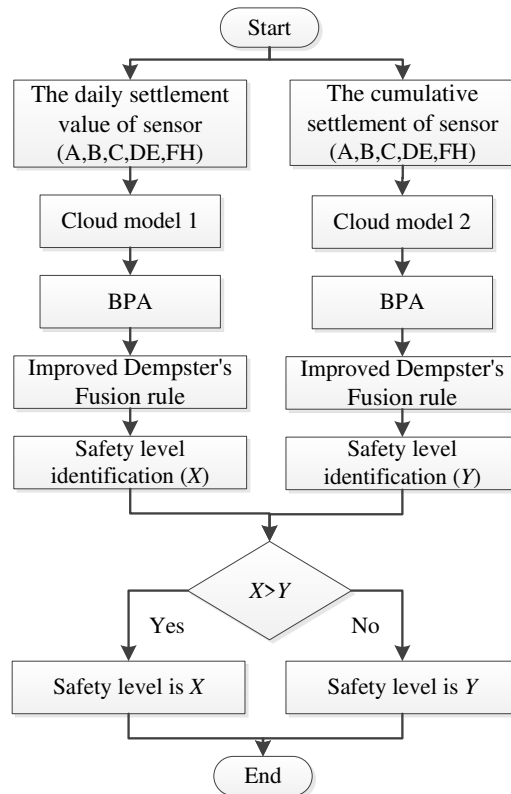
358

of the monitoring data (A, B, C, DE, and FH), and the improved D-S theory is used to fuse them

359 separately to obtain the risk level. Finally, the maximum value of the two result is selected as the
 360 collapse risk value, the flowchart as shown in Fig. 6.

361 **Table 6 Cloud models parameter value of the two monitoring indicators.**

Indicators	I			II			III			IV		
	<i>Ex</i>	<i>En</i>	<i>He</i>									
Daily settlement	1	0.333	0.002	3.5	0.5	0.002	7.5	0.833	0.002	12.5	0.833	0.002
Cumulative settlement	25	8.333	0.002	75	8.333	0.002	150	16.777	0.002	250	16.777	0.002



362

363

Fig. 6 Flowchart of monitoring data processing.

364 According to the flowchart shown in Fig. 6, The monitoring data from the above 20 sections

365 were used for collapse risk assessment, the result as shown in Table 7. Obviously, in tunnel sections

366 (No.6 and No.9), the probability of tunnel collapse for class I (0.50) and class II (0.50) is very close,

367 which means that the results are very uncertain. It is difficult to make an accurate judgment on the

368 risk of tunnel collapse.

369

370

Table 7 Results of Cloud model at ten monitoring sections.

Tunnel section	$m(I)$	$m(II)$	$m(III)$	$m(IV)$	$m(\Theta)$	Predicted level	Ture level
No.1	0.52	0.46	0.00	0.00	0.02	I	II
No.2	0.00	0.00	1.00	0.00	0.00	III	III
No.3	0.48	0.50	0.00	0.00	0.02	II	II
No.4	0.00	0.95	0.00	0.00	0.05	II	II
No.5	0.01	0.97	0.00	0.00	0.02	II	II
No.6	0.50	0.50	0.00	0.00	0.00	--	II
No.7	0.00	1.00	0.00	0.00	0.00	II	II
No.8	1.00	0.00	0.00	0.00	0.00	I	I
No.9	0.50	0.50	0.00	0.00	0.00	--	I
No.10	0.00	0.99	0.00	0.00	0.01	II	I
No.11	0.41	0.53	0.00	0.00	0.06	II	II
No.12	0.00	0.60	0.35	0.00	0.05	II	III
No.13	0.96	0.00	0.00	0.00	0.04	I	I
No.14	1.00	0.00	0.00	0.00	0.00	I	I
No.15	0.03	0.90	0.00	0.00	0.07	II	II
No.16	0.58	0.40	0.00	0.00	0.02	II	I
No.17	0.00	0.93	0.00	0.04	0.03	II	II
No.18	1.00	0.00	0.00	0.00	0.00	I	I
No.19	0.98	0.00	0.00	0.00	0.02	I	I
No.20	0.00	1.00	0.00	0.00	0.00	II	II

371 **5.4 Multi-source information fusion**

372 In order to settle the problem of unreliable evaluation results of single-information sources, the
373 improve D-S evidence theory (Section 2.4) is used to fuse the multi-source data. This method
374 combines the different results of the three above-mentioned single-source assessment methods.
375 According to Eq. (9) and Eq. (10), the fusion results can be calculated, the result as shown in Table
376 8. The following conclusions can be obtained:

377 (1) The multiple-information fusion method proposed in this paper can improve the accuracy
378 and reduce uncertainty in the tunnel collapse risk evaluation. Only section evaluation error appears
379 at section No. 9, indicating that the evaluation accuracy rate of 20 sections has reached 95%. The
380 confidence indexes $m(\Theta)$ of the 20 tunnel sections are all close to 0, which means that the uncertainty

381 of the results is 0.

382 (2) The proposed method can solve the problem of inconsistent results of the three risk
383 assessment methods effectively. For example, because the results of the three risk categories are
384 different (SVM and CM belong to level I and BN belong to level II), the single-source risk
385 assessment method cannot directly assess the overall tunnel collapse risk level of the monitoring
386 section 4. The multi-source information fusion method is used to evaluate the monitoring section 4
387 and the results are shown in Table 8. The BPAs value of tunnel collapse risk level II (that is $m(II)$)
388 is equal to 1, which means that the collapse risk level for the monitoring section 4 is level II with a
389 high confidence level

390 (3) Among those sections, the collapse risk values of sections No.2 and No.12 are III (Small-
391 scale collapse), and the rest are level I (Safe) or level II (Deformation). This indicates that small
392 collapses are likely to occur in sections No.2 and No.12 during the excavation stage. It is necessary
393 to strengthen support levels and supervision to reduce the risk of collapse.

394 **Table 8 Results of multi-source information fusion at ten monitoring sections.**

Tunnel section	$m(I)$	$m(II)$	$m(III)$	$m(IV)$	$m(\Theta)$	Predicted level	Ture level
No.1	0.00	0.99	0.01	0.00	0.00	II	II
No.2	0.00	0.00	1.00	0.00	0.00	III	III
No.3	0.00	1.00	0.00	0.00	0.00	II	II
No.4	0.00	1.00	0.00	0.00	0.00	II	II
No.5	0.00	1.00	0.00	0.00	0.00	II	II
No.6	0.00	1.00	0.00	0.00	0.00	II	II
No.7	0.00	1.00	0.00	0.00	0.00	II	II
No.8	1.00	0.00	0.00	0.00	0.00	I	I
No.9	0.17	0.83	0.00	0.00	0.00	II	I
No.10	0.85	0.11	0.02	0.02	0.00	I	I
No.11	0.00	1.00	0.00	0.00	0.00	II	II
No.12	0.00	0.35	0.64	0.01	0.00	III	III
No.13	1.00	0.00	0.00	0.00	0.00	I	I
No.14	1.00	0.00	0.00	0.00	0.00	I	I
No.15	0.00	1.00	0.00	0.00	0.00	II	II

No.16	0.88	0.12	0.00	0.00	0.00	I	I
No.17	0.00	1.00	0.00	0.00	0.00	II	II
No.18	1.00	0.00	0.00	0.00	0.00	I	I
No.19	1.00	0.00	0.00	0.00	0.00	I	I
No.20	0.00	1.00	0.00	0.00	0.00	II	II

395 **5.5 Verification of evaluation results**

396 When the tunnel was excavated to section ZK243+143, the tunnel vault collapsed, as shown in
397 Fig. 7. This is due to the section being in the fracture zone of the surrounding rock and the
398 insufficient strength of the tunnel lining support, resulting in the tunnel collapse. The multi-source
399 information fusion assessment method was applied to this section for collapse risk assessment, the
400 results as shown in Table 8 (No.2 tunnel section). The results indicate that the section is at small-
401 scale collapse risk with a probability of 1. This section is likely to occur a small-scale collapse if the
402 support conditions are not strengthened. The tunneling collapse risk assessment results are
403 consistent with reality, which proves the usefulness of the assessment method in the actual
404 construction process.



405
406

Fig. 7 Tunnel collapse

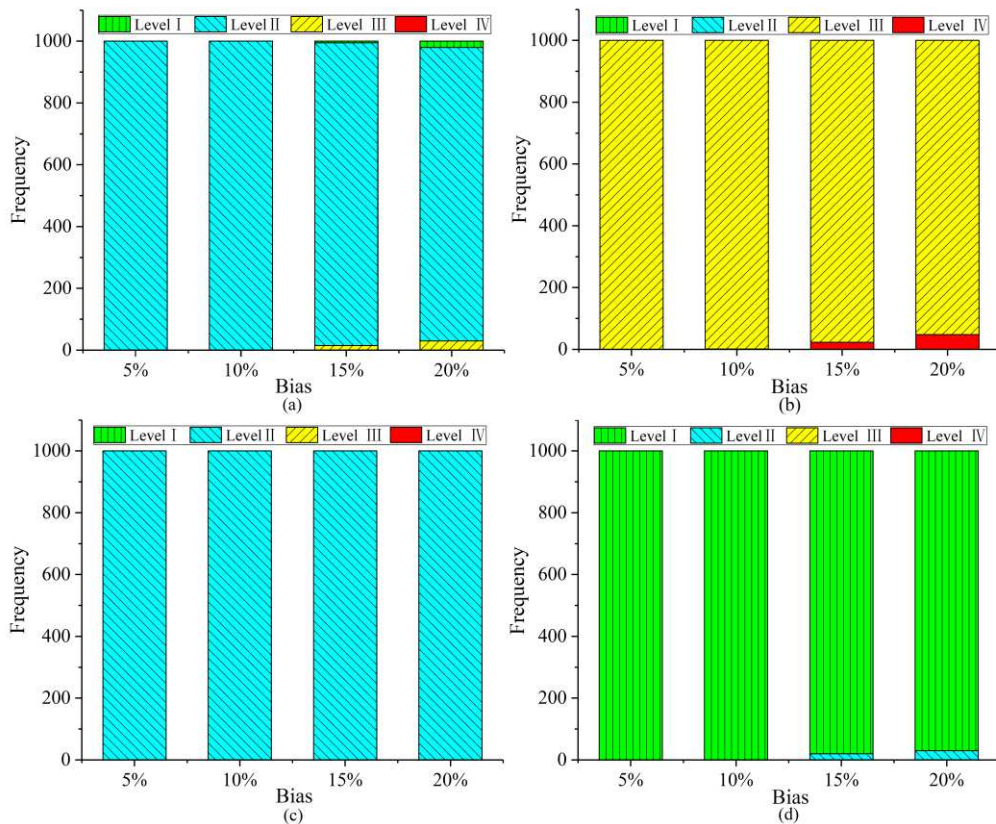
407 5.6 Robustness of risk assessment results

408 In actual engineering, due to the influence of measurement errors and human factors, data from
409 multi-source observations may have inevitable deviations. This article will use the MC simulation
410 technology to simulate the uncertainty of the data. The factors affecting tunnel collapse are assumed
411 to obey normal distribution. To further verify the robustness of the proposed hybrid method under
412 unavoidable deviations, we added different deviation percentages (ie 5%, 10%, 15%, and 20%) to
413 the collected data. In this paper, the number of repeated iterations P is set to 1000. Fig. 8 shows the
414 results of tunnel collapse risk assessment after 1000 iterations for 4 tunnel sections (No. 1, 2, 3, and
415 8) at different offset levels. Fig. 9 shows the global sensitivity analysis about tunnel section No. 2.
416 The following conclusions can be obtained:

417 (1) The proposed multi-source information fusion approach has good robustness to deviation.
418 In order to better understand the bias, Fig. 8 shows the frequency of a certain collapse risk level
419 after 1000 iterations under different biases in 4 tunnel sections (No.1, No.2, No.3, and No.8). When
420 the percentage of bias is increased, the accuracy of the risk assessment will be slightly reduced, but
421 it will remain at a high level. Obviously, all data with a deviation of less than 10% can almost
422 achieve an evaluation accuracy rate close to 100%, proving that the method is accurate and reliable
423 under low bias. When the deviation is 20%, the evaluation accuracy of all tunnel sections is still
424 higher than 90%, which proves that the method has strong robustness under high deviations.
425 Anymore, the accuracy of the assessment of the No. 3 tunnel section under each level of bias has
426 reached 100%. This is because the results of the three single-information evaluation methods of
427 tunnel section No. 3 are consistent (that is, the results of all three different models are risk level II
428 (Deformation)), so no conflicting information will have a negative impact on the result of multi-

429 source information fusion.

430 (2) Since the No. 2 tunnel section is in a dangerous state (Small-scale collapse), a global
431 sensitivity analysis is performed on this part to find out the key risk factors that affect the tunnel
432 collapse. Therefore, some measures to prevent tunnel collapse can be taken in advance. The
433 Spearman's rank correlation coefficient (Eq. (12)) is used to measure the degree of influence of
434 risk factors on the risk level of the tunneling collapse. As shown in Fig. 9, X_3 , X_5 , X_6 , and X_{11} are the
435 top four risk factors that have the greatest impact on tunnel collapse. To reduce the risk level of
436 tunnel section No.2, more attention should be paid to these four risk factors. In addition, when the
437 deviation level increases to 20%, the results of the most sensitive risk factors remain unchanged,
438 again verifying the robustness of the proposed method.

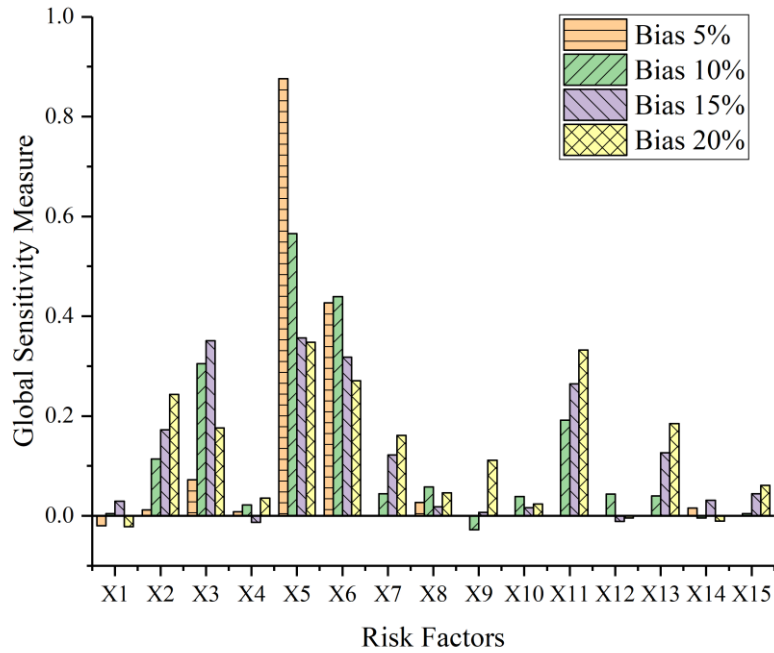


439

440 **Fig. 8 Tunnel collapse risk assessment results after 1000 iterations under different deviation levels at**

441

four section: (a) No.1; (b) No.2; (c) No.3; (d) No.8.



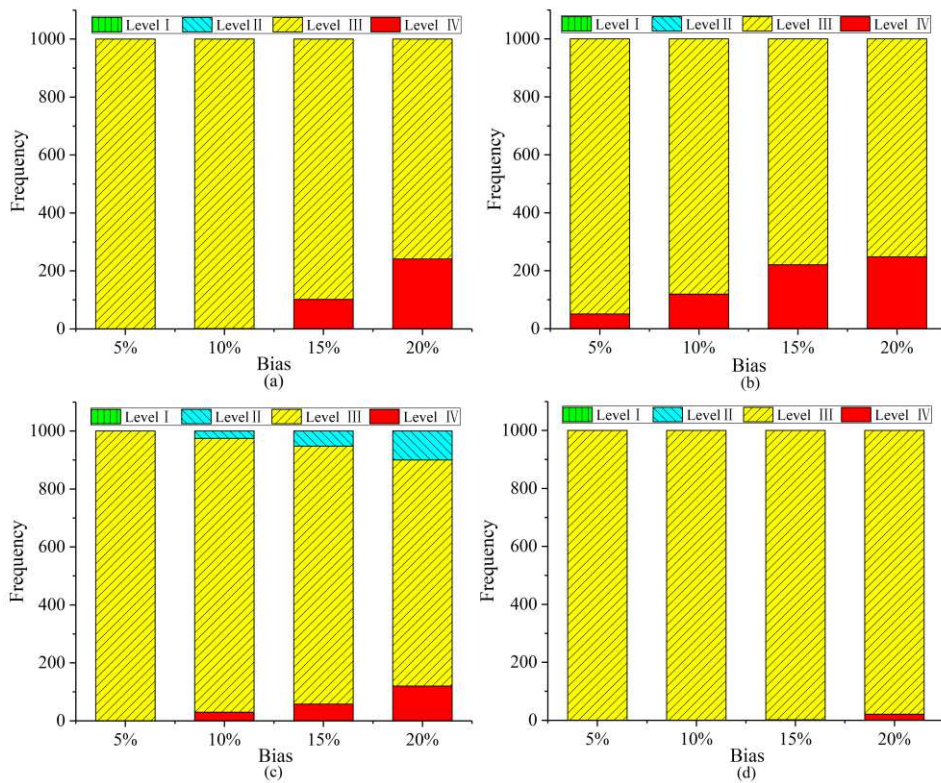
442
443 **Fig. 9 Global sensitivity analysis of 15 risk indicators (No. 2 section)**

444 **4. Discussion**

445 There is no doubt that the single-source information assessment method also can estimate the
 446 tunnel collapse risk level. However, the single source of information does not fully reflect the
 447 environment of the tunnel construction, resulting in a certain bias and low accuracy of the
 448 assessment results. To compare the single-source information evaluation method with the multi-
 449 source information fusion method, the Monte Carlo simulation is used to simulate the inevitable
 450 uncertainty, and the four evaluation methods are calculated 1000 times. The tunneling collapse risk
 451 assessment results of four assessment methods iterate 1000 times under different deviation levels at
 452 tunnel section No.2, as shown in Fig. 10. The following conclusions can be obtained:

453 The single-source information assessment method (Fig. 10 (a), (b), and (c)) can get an accurate
 454 assessment result in case of small deviations, but it performs poorly at high bias. The multi-source

455 information fusion method is more robust than the single-source information assessment method.
 456 As seen in Fig. 10 (d), the multi-source information fusion method has a higher accuracy of
 457 assessment under a large bias, proving that the proposed method has good robustness. This is
 458 because the proposed method makes full use of available information, including contradictory
 459 information. When the data deviation is 20%, the evaluation accuracy of the single-source
 460 information evaluation method is less than 80% in 1000 iterations. In order words, the single-source
 461 information assessment method has a high sensibility to bias. However, the multi-source
 462 information fusion method can still have 97.9% accuracy of assessment in a 20% bias. This method
 463 is a good solution to the data bias caused by the large amount of uncertainty and complexity of the
 464 underground environment.



465
 466 **Fig. 10 Four risk evaluation methods for tunnel collapse risk assessment after 1000 iterations under**
 467 **different deviation levels: (a) SVM; (b) BN; (c) CM; (d) Multi-source information fusion method.**

468 5. Conclusions and future works

469 This paper proposes a multi-source information fusion method for the tunneling collapse risk
470 assessment, which provides risk warning and decision-making suggestions for tunnel excavation.
471 The analysis process consists of four main steps: (1) Risk assessment systems are established for
472 the three information sources (i.e. statistical data, physical sensors, and expert judgment provided
473 by humans) separately; (2) The three information sources are processed by the BN, CM, and SVM
474 respectively to obtain the BPAs of the collapse risk; (3) All predictions from three different
475 assessment method are fused to obtain the overall tunneling collapse risk; (4) The Monte Carlo
476 simulation method is used for global sensitivity analysis and robustness verification. Finally, the
477 Jinzhupa tunnel in China is used to verify the applicability of the proposed approach. The methods
478 developed in this research have the following innovations and capabilities:

479 (1) It can synthesize multi-source information to obtain a more accurate result for the tunneling
480 collapse risk assessment. Due to many risk factors, the tunneling collapse risk assessment is a multi-
481 attribute decision-making problem. In this paper, both soft data from domain experts and hard data
482 from electrical sensors and statistical data are used for evaluating the tunnel collapse risk. A hybrid
483 combination rule combining the weighted mean rule and Dempster's rule is proposed to process
484 multiple conflicting pieces of evidence. Besides, a confidence index, $m(\Theta)$ is adopted to measure
485 the reliability of the tunnel collapse risk result. As shown in Table 8, the value of $m(\Theta)$ is zero,
486 indicating that the tunneling collapse risk has a high degree of confidence.

487 (2) As the deviation level of input data increases, the accuracy rate of the single-source
488 information evaluation method is gradually decreasing. However, the proposed multi-source

489 information fusion method is very robust to deviations. Even when the deviation is 20%, the
490 accuracy of the collapse risk assessment still reaches 97.9%. In other words, this method has
491 excellent tolerance to bias, which eliminates the adverse effects of deviation to the maximum extent
492 and ensures the accuracy and reliability of the evaluation results.

493 (3) When the tunnel section is in a dangerous state, in order to provide advice to decision-
494 makers, global sensitivity analysis is proposed to identify the most influential risk factors. The
495 global sensitivity analysis considers the interaction between risk factors, making the results more in
496 line with actual construction conditions. In the tunnel case of this study, the factors X_3 (Rock mass
497 grade), X_5 (Unfavorable geology), X_6 (Bias angle), and X_{11} (Timeliness of primary support) are
498 identified to have the greatest impact on the risk of tunnel collapse. Besides, because measurement
499 errors or human errors may cause data deviations, the MC method is used to simulate the data
500 deviations to prove that the proposed method still has good robustness under deviations.

501 The proposed method in this paper also has some limitations. Experts are still required to
502 participate in the entire evaluation process, which means that a truly automated evaluation has not
503 yet been achieved. In terms of tunnel collapse data collection, the amount of data is still small, and
504 a system needs to be developed to collect data on a global scale. In addition, this method cannot
505 predict the risk status of the next construction process, and further research is needed.

506 **Data Availability Statement**

507 The datasets generated during and/or analyzed during the current study are not publicly
508 available but are available from the corresponding author on reasonable request.

509 **Acknowledgments**

510 This work was supported by the National Natural Science Foundation of China (Grant Nos.:
511 51678164; 51478118); Guangxi Natural Science Foundation (Grant Nos.: 2018GXNSFDA138009).

512 The authors would like to express the appreciation and thanks to the managers and San-Ming
513 Pu-Yan Expressway Co. LTD.

514 **Conflicts of Interest**

515 The authors declare no conflicts of interest.

516

517

518 **References**

- 519 Balazs, J.A., Velásquez, J.D., 2016. Opinion Mining and Information Fusion: A survey. *Information*
520 *Fusion* 27, 95–110. <https://doi.org/10.1016/j.inffus.2015.06.002>
- 521 Ding, L.Y., Zhou, C., 2013. Development of web-based system for safety risk early warning in urban
522 metro construction. *Automation in Construction* 34, 45–55.
523 <https://doi.org/10.1016/j.autcon.2012.11.001>
- 524 Guo, K., Zhang, L., 2021. Multi-source information fusion for safety risk assessment in underground
525 tunnels. *Knowledge-Based Systems* 227, 107210.
526 <https://doi.org/10.1016/j.knosys.2021.107210>
- 527 Haroonabadi, H., Haghifam, M.-R., 2011. Generation reliability assessment in power markets using
528 Monte Carlo simulation and soft computing. *Applied Soft Computing* 11, 5292–5298.
529 <https://doi.org/10.1016/j.asoc.2011.05.031>
- 530 Hasanpour, R., Rostami, J., Schmitt, J., Ozcelik, Y., Sohrabian, B., 2020. Prediction of TBM
531 jamming risk in squeezing grounds using Bayesian and artificial neural networks. *Journal of*
532 *Rock Mechanics and Geotechnical Engineering* 12, 21–31.
533 <https://doi.org/10.1016/j.jrmge.2019.04.006>
- 534 Huang, Y., 2009. *Advances in Artificial Neural Networks – Methodological Development and*
535 *Application*. *Algorithms* 2, 973–1007. <https://doi.org/10.3390/algorithm2030973>
- 536 Janssen, H., 2013. Monte-Carlo based uncertainty analysis: Sampling efficiency and sampling
537 convergence. *Reliability Engineering & System Safety* 109, 123–132.
538 <https://doi.org/10.1016/j.res.2012.08.003>

539 Kou, G., Lu, Y., Peng, Y., Shi, Y., 2012. Evaluation of classification algorithms using mcdm and
540 rank correlation. *Int. J. Info. Tech. Dec. Mak.* 11, 197–225.
541 <https://doi.org/10.1142/S0219622012500095>

542 Leung, Y., Ji, N.-N., Ma, J.-H., 2013. An integrated information fusion approach based on the theory
543 of evidence and group decision-making. *Information Fusion* 14, 410–422.
544 <https://doi.org/10.1016/j.inffus.2012.08.002>

545 Li, D., Liu, C., Gan, W., 2009. A new cognitive model: Cloud model. *Int. J. Intell. Syst.* 24, 357–
546 375. <https://doi.org/10.1002/int.20340>

547 Li, N., Feng, X., Jimenez, R., 2017. Predicting rock burst hazard with incomplete data using
548 Bayesian networks. *Tunnelling and Underground Space Technology* 61, 61–70.
549 <https://doi.org/10.1016/j.tust.2016.09.010>

550 Li, S., Liu, C., Zhou, Z., Li, L., Shi, S., Yuan, Y., 2021. Multi-sources information fusion analysis
551 of water inrush disaster in tunnels based on improved theory of evidence. *Tunnelling and*
552 *Underground Space Technology* 113, 103948. <https://doi.org/10.1016/j.tust.2021.103948>

553 Liu, K., Liu, B., 2019. Intelligent information-based construction in tunnel engineering based on the
554 GA and CCGPR coupled algorithm. *Tunnelling and Underground Space Technology* 88, 113–
555 128. <https://doi.org/10.1016/j.tust.2019.02.012>

556 Liu, Y., Lian, J., Bartolacci, M.R., Zeng, Q.-A., 2014. Density-Based Penalty Parameter
557 Optimization on C-SVM. *The Scientific World Journal* 2014, 1–9.
558 <https://doi.org/10.1155/2014/851814>

559 Pan, Y., Zhang, L., 2021. Roles of artificial intelligence in construction engineering and management:
560 A critical review and future trends. *Automation in Construction* 122, 103517.

561 <https://doi.org/10.1016/j.autcon.2020.103517>

562 Pan, Y., Zhang, L., Wu, X., Skibniewski, M.J., 2020. Multi-classifier information fusion in risk
563 analysis. *Information Fusion* 60, 121–136. <https://doi.org/10.1016/j.inffus.2020.02.003>

564 Qian, Y., Liang, J., Yao, Y., Dang, C., 2010. MGRS: A multi-granulation rough set. *Information
565 Sciences, Special Issue on Modelling Uncertainty* 180, 949–970.
566 <https://doi.org/10.1016/j.ins.2009.11.023>

567 Qiao, S., Cai, Z., Tan, J., Xu, P., Zhang, Y., 2020. Analysis of Collapse Mechanism and Treatment
568 Evaluation of a Deeply Buried Hard Rock Tunnel. *Applied Sciences* 10, 4294.
569 <https://doi.org/10.3390/app10124294>

570 Robert, C.P., Casella, G., 2004. *Monte Carlo Statistical Methods*, Springer Texts in Statistics.
571 Springer New York, New York, NY. <https://doi.org/10.1007/978-1-4757-4145-2>

572 Satpal, S.B., Guha, A., Banerjee, S., 2016. Damage identification in aluminum beams using support
573 vector machine: Numerical and experimental studies: *Damage Identification in Al Beams
574 Using SVM: Numerical and Exp Studies. Struct. Control Health Monit.* 23, 446–457.
575 <https://doi.org/10.1002/stc.1773>

576 Wang, B., Li, S., Zhang, Qianqing, Li, L., Zhang, Qian, Xu, F., 2016. Risk Assessment of a Tunnel
577 Collapse in a Mountain Tunnel Based on the Attribute Synthetic Evaluation System, in: *Geo-
578 China 2016. Presented at the Fourth Geo-China International Conference, American Society of
579 Civil Engineers, Shandong, China*, pp. 198–209. <https://doi.org/10.1061/9780784480038.025>

580 Wang, S., Li, L., Shi, S., Cheng, S., Hu, H., Wen, T., 2020. Dynamic Risk Assessment Method of
581 Collapse in Mountain Tunnels and Application. *Geotech Geol Eng* 38, 2913–2926.
582 <https://doi.org/10.1007/s10706-020-01196-7>

583 Worden, K., Manson, G., 2007. The application of machine learning to structural health monitoring.
584 Phil. Trans. R. Soc. A. 365, 515–537. <https://doi.org/10.1098/rsta.2006.1938>

585 Wu, X., Liu, H., Zhang, L., Skibniewski, M.J., Deng, Q., Teng, J., 2015. A dynamic Bayesian
586 network based approach to safety decision support in tunnel construction. Reliability
587 Engineering & System Safety 134, 157–168. <https://doi.org/10.1016/j.res.2014.10.021>

588 Yager, R.R., 2016. Multi-source Information Fusion Using Measure Representations, in: Saminger-
589 Platz, S., Mesiar, R. (Eds.), On Logical, Algebraic, and Probabilistic Aspects of Fuzzy Set
590 Theory, Studies in Fuzziness and Soft Computing. Springer International Publishing, Cham,
591 pp. 199–214. https://doi.org/10.1007/978-3-319-28808-6_12

592 Zhang, G.-H., Chen, W., Jiao, Y.-Y., Wang, H., Wang, C.-T., 2020. A failure probability evaluation
593 method for collapse of drill-and-blast tunnels based on multistate fuzzy Bayesian network.
594 Engineering Geology 276, 105752. <https://doi.org/10.1016/j.enggeo.2020.105752>

595 Zhang L, Wu X, Mirosław J, et al. Bayesian-Network-Based Safety Risk Analysis in Construction
596 Projects[J]. Reliability Engineering & System Safety, 2014, 131: 29-39.
597 <https://doi.org/10.1016/j.res.2014.06.006>

598 Zhang, L., Wu, X., Zhu, H., AbouRizk, S.M., 2017. Perceiving safety risk of buildings adjacent to
599 tunneling excavation: An information fusion approach. Automation in Construction 73, 88–
600 101. <https://doi.org/10.1016/j.autcon.2016.09.003>

601 Zhang, P., Li, T., Wang, G., Luo, C., Chen, H., Zhang, J., Wang, D., Yu, Z., 2021. Multi-source
602 information fusion based on rough set theory: A review. Information Fusion 68, 85–117.
603 <https://doi.org/10.1016/j.inffus.2020.11.004>

604 Zhou, C., Yin, K., Cao, Y., Ahmed, B., 2016. Application of time series analysis and PSO–SVM

605 model in predicting the Bazimen landslide in the Three Gorges Reservoir, China. *Engineering*
606 *Geology* 204, 108–120. <https://doi.org/10.1016/j.enggeo.2016.02.009>

607 Zhou, F., 2008. *Research on Fuzzy Hierarchical Evaluation of Mountain Tunnel Landslide Risk*.
608 Master's Thesis, Central South University, China, Changsha

609 Sun, J., 2019. *Study on collapse risk and stability evaluation in mining construction of mountain*
610 *tunnel*. Master's Thesis, Beijing Jiaotong University, China, Beijing

611 JTG/T 3660-2020. *Technical specification for construction of highway tunnel*

612 DB 35/T 1067-2010. *Technical code for monitoring measurement of highway tunnel*

613

614